



Enhanced ferroelectricity for nanoporous barium titanate: a phase-field prediction

Chengmin Xie^{a,b}, He Zhao^{a,b}, Lifei Du^c, Huiling Du^c and Pingping Wu ^{a,b}

^aDepartment of Materials Science and Engineering, Xiamen Institute of Technology, Xiamen, People's Republic of China; ^bThe Higher Educational Key Laboratory for Flexible Manufacturing Equipment Integration of Fujian Province, Xiamen Institute of Technology, Xiamen, People's Republic of China; ^cCollege of Materials Science and Engineering, Xi'an University of Science and Technology, Xi'an, People's Republic of China

ABSTRACT

Porous ferroelectric materials show great potential for achieving competitive dielectric/piezoelectric properties with light weight. In this study, a phase-field model was employed to simulate the ferroelectric domain structure evolution of porous barium titanate. It is suggested that the ferroelectric/dielectric/piezoelectric properties are strongly influenced by the porosity level and the size of pores for porous ceramics. It is demonstrated that the ferroelectric switching behaviour, the remnant polarisation, the dielectric constant and the piezoelectric constant are enhanced in nanoporous ferroelectrics with ellipse-shaped pores by introducing mechanisms of symmetry breaking. By providing a means of achieving enhanced properties, nanoporous ferroelectrics with ellipse-shaped pores may have a broad impact on the applications of ferroelectrics and enhance the utility of the materials for selected applications.

ARTICLE HISTORY

Received 4 January 2021
Accepted 18 May 2021

KEYWORDS

Ferroelectric; nanoporous; BaTiO₃; phase-field model

1. Introduction

Introducing pores into a dense ferroelectric is an effective way of controlling its ferroelectric/piezoelectric properties [1, 2]. For energy harvest application [3], permittivity is reduced owing to the introduction of low-permittivity pores, which have beneficial consequences for piezo- and pyro-electric energy harvesting as the porous piezoelectric and pyroelectric materials can be considered as a porosity (air) – ceramic matrix composite. Furthermore, porous ferroelectric materials show potential for achieving competitive dielectric/piezoelectric properties combined with light weight, and the reduced permittivity can lead to improvement in the sensor/harvesting figures of merit of ferroelectrics[4]. Recently, great interest in nanostructural/nanoscale porous ferroelectric materials has been driven by the

CONTACT Pingping Wu  pingpingwu-ustb@126.com  Department of Materials Science and Engineering, Xiamen Institute of Technology, Xiamen, Fujian 361021, People's Republic of China; The Higher Educational Key Laboratory for Flexible Manufacturing Equipment Integration of Fujian Province, Xiamen Institute of Technology, Xiamen, Fujian 361021, People's Republic of China

great potential of these porous ferroelectrics in various applications, including traditional dielectric/piezoelectric applications [5–8], PVDF (polyvinylidene fluoride) film based memory devices [9], and some magnetoelectronic applications [10, 11].

In another aspect, the connectivity and alignment of pores have been investigated for porous ferroelectrics. Ronit Kar-Gupta et al. [12] developed a model to predict 3–1 type porous piezoelectric materials with ‘longitudinally’ porous and ‘transversely’ porous arrangements. Zhang et al. [3] discovered that aligned porosity in PZT (lead zirconate titanate) reduces the values of both permittivity and specific heat capacity. Castro et al. [13] introduced nanopores into dense ferroelectric PbTiO_3 thin films to improve tetragonality and showed enhancement in piezoelectric coefficients and switchable polarisation with a low local coercive field. Khachatryan et al. [14] studied polarisation-switching dynamics in bulk ferroelectrics with isometric and oriented anisometric pores. Ming et al. [15] simulated isolated pores and connected pores in $\text{Pb}(\text{Mg}_{1/3}\text{Nb}_{2/3})\text{O}_3$ - PbTiO_3 (PMN-PT), with the connected-pore structure exhibiting a lower piezoelectric coefficient than the structure-containing isolated pores. Zhang et al. [16] combined experimental and modelling studies to provide a detailed examination of the influence of porosity volume fraction and morphology on the polarisation/electric field response of ferroelectric materials. Martínez-Ayuso et al. [17] proposed a finite-element model to perform a detailed study of the influence of polarisation, electric field, and geometry of the inclusions on the piezoelectric and dielectric coefficients of porous piezoelectric ceramics. Very recently, Van Lich et al. [18] investigated the topological polarisation structures of nanoporous ferroelectrics, as well as the electromechanical response and electrocaloric properties of nanostructured ferroelectrics with geometric configurations investigated by simulation works of Chen et al [19] and Hou et al [20]. Khan et al [21] and Shu et al [22] designed highly porous mechanical metamaterials by introducing micro-architectures to improve the properties of porous ferroelectrics. Roscow et al. [23] reported that enhancement in piezoelectric energy harvesting of barium titanate can be achieved by forming highly aligned porosity with freeze-casting technology.

Our previous work [24] simulated structures and properties of porous ferroelectrics with various shaped pores. However, these simulations focussed on the ferroelectric part of the materials and neglected the interface effect of the pores, i.e. a sharp interface was introduced in the simulation. In our current work, we employed the phase-field model to predict the evolution of the ferroelectric domain structures and the porous phase structures simultaneously. The lead-free ferroelectric barium titanate (BaTiO_3) was chosen for our simulations owing to its high dielectric constant and low breakdown strength. We find that the ferroelectric/dielectric/piezoelectric properties of porous BaTiO_3 can easily be adjusted by controlling the porosity and the pore diameter. Finally, we found an enhanced dielectric/piezoelectric d_{33} by elongating the shape of the pores. Ellipse-shaped pores can significantly improve the ferroelectric properties. The porosity offers a competitive potential compared to dense ferroelectrics.

2. Simulation method

In this work, in order to simulate the evolution of ferroelectric domain structures with the introduction of pores, we chose two order parameters: the electrical polarisation $P_i = 1, 2, 3$, describing the ferroelectric domains, and an order parameter η , describing the pore phase in the ferroelectrics. Thus, the structures of the materials can be described by the following equations:

$$\frac{\partial P_i(r, t)}{\partial t} = -L_p \frac{\delta F}{\delta P_i(r, t)} \quad (1)$$

$$\frac{\partial \eta(r, t)}{\partial t} = -L_\eta \frac{\delta F}{\delta \eta(r, t)} \quad (2)$$

where L_p and L_η are kinetic parameters, r is a Cartesian coordinate, t is time, and F is the total free energy of the system:

$$F = \int_V [\eta(r)f_{\text{pore}} + (1 - \eta(r))f_{\text{electric}}]dV \quad (3)$$

where f_{pore} is the energy contribution of the pore phase to the total free energy, which was assumed to be zero in this work. f_{electric} is the contribution of the ferroelectric phase. When substituting the total free energy F into (1), we take the partial derivative of the free energy with respect to polarisation, while the other order parameter η was held constant. In the same way, when substituting F into (2), we do a partial derivative of free energy with respect to η , holding the polarisation P constant. Thus, simultaneous solving of equations (1) and (2), one can achieve the evolution of the ferroelectric polarisation distribution and the pore phase structure.

In the total free energy of regular ferroelectrics, the Landau free energy, the interfacial energy, the electric energy and the elastic energy, are represented by f_{land} , f_{inter} , f_{elec} and f_{elas} , respectively. Thus, the total free energy can be expressed by

$$\begin{aligned} F &= \int_V [\eta(r)f_{\text{pore}} + (1 - \eta(r))f_{\text{electric}}]dV \\ &= \int_V [\eta(r)f_{\text{pore}} + (1 - \eta(r)) \cdot (f_{\text{land}} + f_{\text{inter}} + f_{\text{elec}} + f_{\text{elas}})]dV \\ &= \int_V [\eta(r)f_{\text{pore}} + (1 - \eta(r)) \cdot \left(\frac{1}{2} \alpha_{ij} P_i P_j + \frac{1}{4} \beta_{ijkl} P_i P_j P_k P_l + \dots + \frac{1}{2} G_{ijkl} \frac{\partial P_i}{\partial x_j} \frac{\partial P_k}{\partial x_l} \right. \\ &\quad \left. + \left(-\frac{1}{2} \varepsilon_b \varepsilon_0 E_i^2 - E_i P_i \right) + \frac{1}{2} C_{ijkl} (\varepsilon_{ij} - Q_{ijkl} P_k P_l) (\varepsilon_{kl} - Q_{kl ij} P_i P_j) \right)]dV \end{aligned} \quad (4)$$

where α_{ij} , β_{ijkl} ... are Landau expansion coefficients, G_{ijkl} is the gradient energy coefficient, ϵ_0 is the vacuum permittivity, ϵ_b is the background relative dielectric permittivity, E_i is the external electric field, C_{ijkl} is the elastic stiffness tensor, ϵ_{ij} is the total strain and Q_{ijkl} represents the electrostrictive coefficient. Khachaturyan's elastic theory [25] is employed to solve for the elastic energy term f_{elas} .

3. Results and discussion

BaTiO₃ is taken as the aim material in this work. The corresponding coefficients in our simulation are [24]: $\alpha_1 = 4.124(T - 388) \times 10^5$, $\alpha_{11} = -2.097 \times 10^8$, $\alpha_{12} = 7.974 \times 10^8$, $\alpha_{111} = 1.294 \times 10^9$, $\alpha_{112} = -1.905 \times 10^9$, $\alpha_{123} = 2.500 \times 10^9$, $\alpha_{1111} = 3.863 \times 10^{10}$, $\alpha_{1112} = 2.529 \times 10^{10}$, $\alpha_{1122} = 1.637 \times 10^{10}$, $\alpha_{1123} = 1.367 \times 10^{10}$, $C_{11} = 1.78 \times 10^{11}$, $C_{12} = 0.964 \times 10^{11}$, $C_{44} = 1.22 \times 10^{11}$, $Q_{11} = 0.10$, $Q_{12} = -0.034$, $Q_{44} = 0.029$. For simplify, the kinetic coefficient L_p and L_η are chosen to be 1.0. All the units for the parameters are in SI unit and T is in Kelvin. Room temperature of 298.15 K is used in our current simulation.

For comparison and validation, we use the following two types of interfaces to describe the ferroelectric domain structure in the numerical simulation. Figure 1(a) and (b) show the ferroelectric domain structure with a sharp interface and a diffuse interface, respectively. A circle-shaped pore with a radius of 32 nm was placed at the centre of bulk BaTiO₃ with a 128×128 computational grid. The polarisation is initially polarised along the [001] direction. We examined the order parameter η and the ferroelectric polarisation P along the dashed line in the x direction and passing through the centre of the circle, as shown in Figure 1(c) and (d). As one can see, the diffuse interface leads to a gradual change in the polarisation across the interface, while a sharp interface leads to a rapid change in polarisation. In the case of the diffuse interface, the value of η undergoes a gradual change instead of discontinuous jump. However, the polarisation near the interfaces is reduced on account of an electrostatic effect, which makes the size of the pores a little bit larger in the domain configuration.

In order to investigate the effects of the pore size and the porosity on the ferroelectrics, we performed three groups of ferroelectrics with pore radii of 16, 32 and 64 nm, and adjusted the porosity level from 50% to 5%. The size of the simulated nanopores is close to those observed experimentally in a nanowire structure by Kvasov et al. [5] In the simulation, as a periodical boundary condition is employed along the x-y direction, we kept the pore radius constant and increased the distance between the pores to decrease the porosity of the materials. Figure 2 shows the ferroelectric domain structures of nanoporous BaTiO₃ at different porosity levels. It can be seen that the size of the pores is close to the ferroelectric domain size in the simulation. The yellow/orange/green/dark green coloured domains in the images correspond to domains in

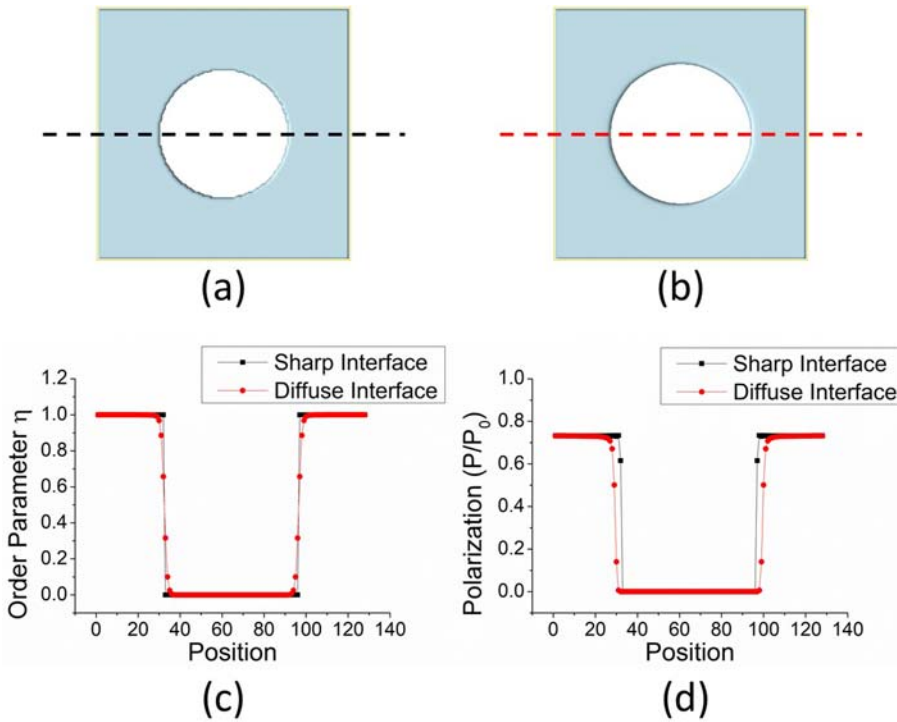


Figure 1. (a, b) Simulated ferroelectric domain structures with a circle-shaped pore located at the centre of a polarised ferroelectric. Sharp and diffuse interfaces were employed in the simulation. (c) Calculated order parameter η and (d) polarisation P along the horizontal dashed line in (a, b); black squares: sharp interface; red circles: diffuse interface.

which the polarisation is oriented towards $+x/-x/+y/-y$ directions, respectively. The light blue/blue coloured boundaries between the domains represent the ferroelectric domain walls in which the polarisation is oriented towards the $+z/-z$ direction. For all the nanoporous domain structures, stripe domains were observed in the microstructures. Similar to those in dense ferroelectrics, these stripes are separated by 90-degree domain walls and, inside the stripes, the domains can be divided into two types of anti-parallel domains with 180-degree domain walls. This complex structure with 90-degree and 180-degree walls can be seen clearly, especially for the ferroelectrics having low porosity levels and large pore radii. If many small pores occupy the space of the ferroelectric phase, i.e. a material with a high porosity level and small pore radius, small tetragonal microdomains form around the pores. As the porosity of the ceramics is close to the upper limit that theory permits and when the pore radius is very small, this structure is difficult to be observed in experimentally.

Since new interfaces are introduced by the pores, in order to minimise the electrostatic energy of depolarisation fields in the system, ferroelectric domains try to avoid the formation of a residual surface charge near the pores. i.e. the direction of polarisation is parallel to the tangent plane to the

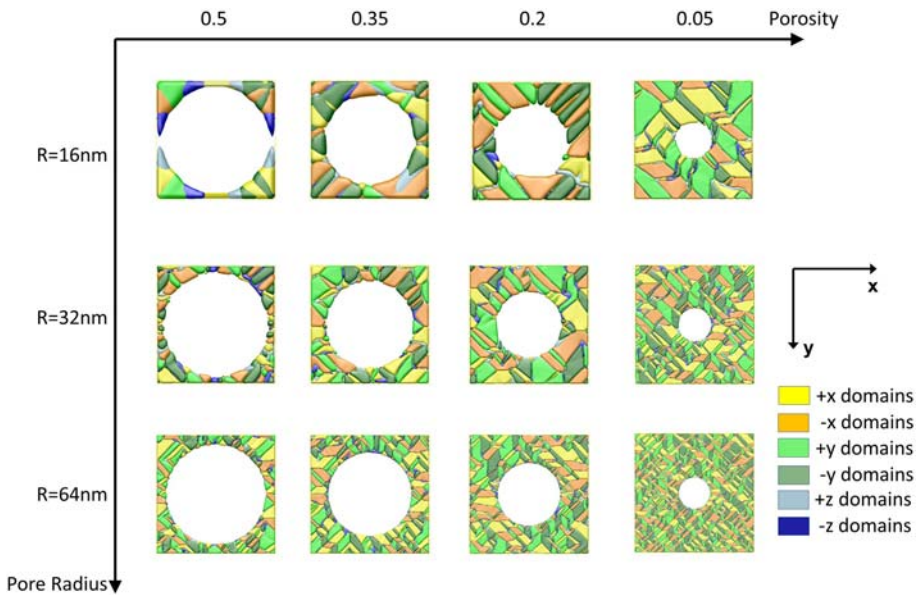


Figure 2. Ferroelectric domain structures at zero external field for various pore porosity values from 0.5 to -0.05 and pore radii from 16 to 64 nm.

pore surface. With an increase in the simulation size, the size of the domains cannot elongate at the same time, as the elastic strain energy term is added to the total free energy, which is proportional to the volume of the domains. The elastic energy is lowered by reducing the size of the domains, which in turn requires smaller domains. Although small domains introduce additional domain wall energy, they reduce the electrostatic energy and the total free energy of the system as a consequence.

Figure 3 illustrates the PE loops for the porous BaTiO_3 with different porosities in the range 0.5–0.05. Since in this work periodic boundary conditions along the x - and y -directions are employed, we focus with the model only on predicting porous ferroelectric properties, including a single pore structure. For comparison, hysteresis loops of a four-pore structure were performed, for which the result is very similar to that of a one-pore structure. In Figure 3, the black-square, red-circle, and blue-triangle-shaped symbols represent the loops of the materials with round pores with radii of 16 nm, 32 nm, 64 nm, respectively. The remanent polarisation (P_r) of high-porosity samples is lower than that of low-porosity samples owing to the reduced amount of ferroelectric phase. Moreover, the increase of the pore size leads to a higher remanent polarisation P_r , which can be explained by the pinning of the domain walls. For the ceramics with a specific porosity, large pores imply an increase in the volume fraction of domain walls and increase the difficulty of domain wall movement. Similarly, the coercive field of high-porosity BaTiO_3 is low compared to that of the BaTiO_3 with low porosity, but the coercive field of

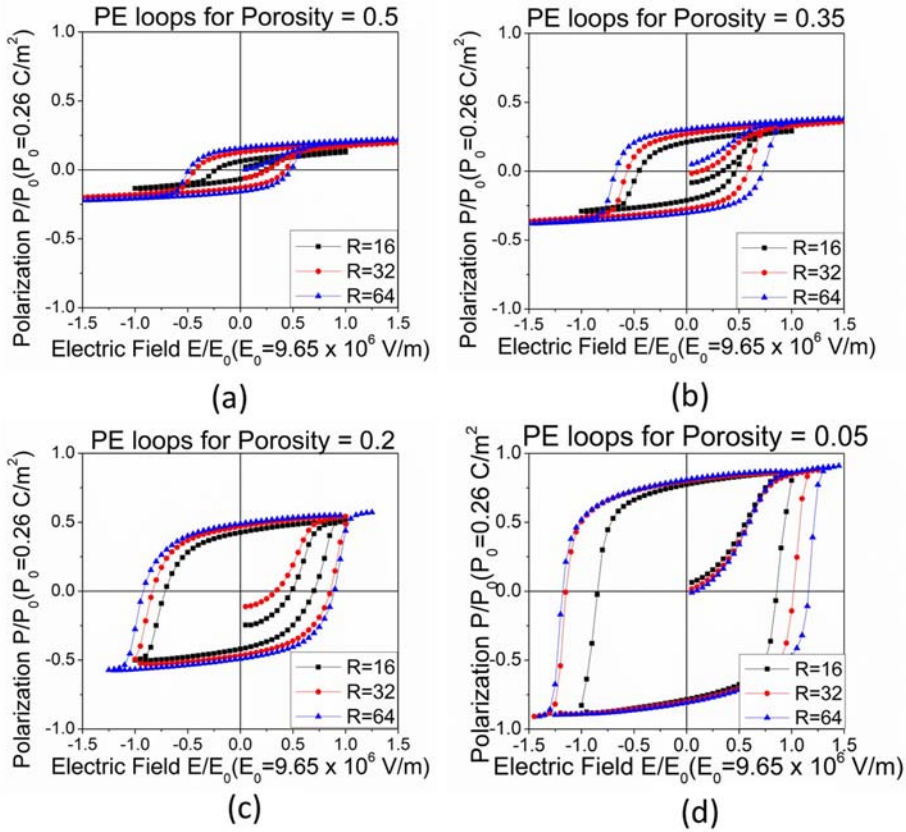


Figure 3. Simulated ferroelectric hysteresis loops of porous BaTiO₃ at porosity levels of (a) 0.5%, (b) 0.35%, (c) 0.2% and (d) 0.05%, where black squares, red dots, blue triangles represent ferroelectrics with pore radii of 16, 32 and 64 nm, respectively.

the ceramics with a large pore size is high compared to that of the ferroelectrics with a small pore radius. The increase in the coercive field for large pore size is caused by the depolarisation field, which is generated from two neighbouring pore surfaces. At the same porosity level, large pores mean that the spacing between the pores is also large, which reduces the depolarisation field between the two pore surfaces. A lower depolarisation field makes polarisation switching much more difficult, and increases the coercive field of the hysteresis loop.

Figure 4(a–d) shows the remanent polarisation P_r/P_0 , the rectangularity factor P_r/P_s , the dielectric constant ϵ_{33} and the piezoelectric coefficient d_{33} versus porosity for porous BaTiO₃. It can be seen that, after the introduction of porosity, the P_r value decreases very fast in the porosity range from 0.05–0.2. In contrast, the rectangularity factor P_r/P_s undergoes minor changes during this initial stage, while there is a significant decrease in this factor in high-porosity ceramics with a pore size of 64 nm. The properties of ferroelectrics are strongly diminished by the polarisation saturation P_s associated with

high porosity, suggesting limited applications of the ferroelectrics with large size pores. In addition, pores reduce the dielectric constant and the piezoelectric constant d_{33} further limiting applications of high-porosity ferroelectrics.

It is possible to improve ferroelectric properties of fixed porosity. Lightweight ferroelectrics with competitive dielectric and piezoelectric properties offer the possibility of decreasing the cost and mass of such materials. According to previous studies [12, 14–16, 23], a possible way to enhance ferroelectric/piezoelectric properties is to elongate the shape of the pores. In this study, we simulated the domain structure and the hysteresis loops of BaTiO₃ with ellipse-shaped pores. In our previous work [24], it has been shown that broken symmetry can lead to the enhancement of ferroelectric properties, including remanent polarisation, dielectric constant, and piezoelectric parameters.

We can understand the mechanism of enhancement from the ferroelectric domain configurations. Figure 5 presents the hysteresis loops of BaTiO₃ with

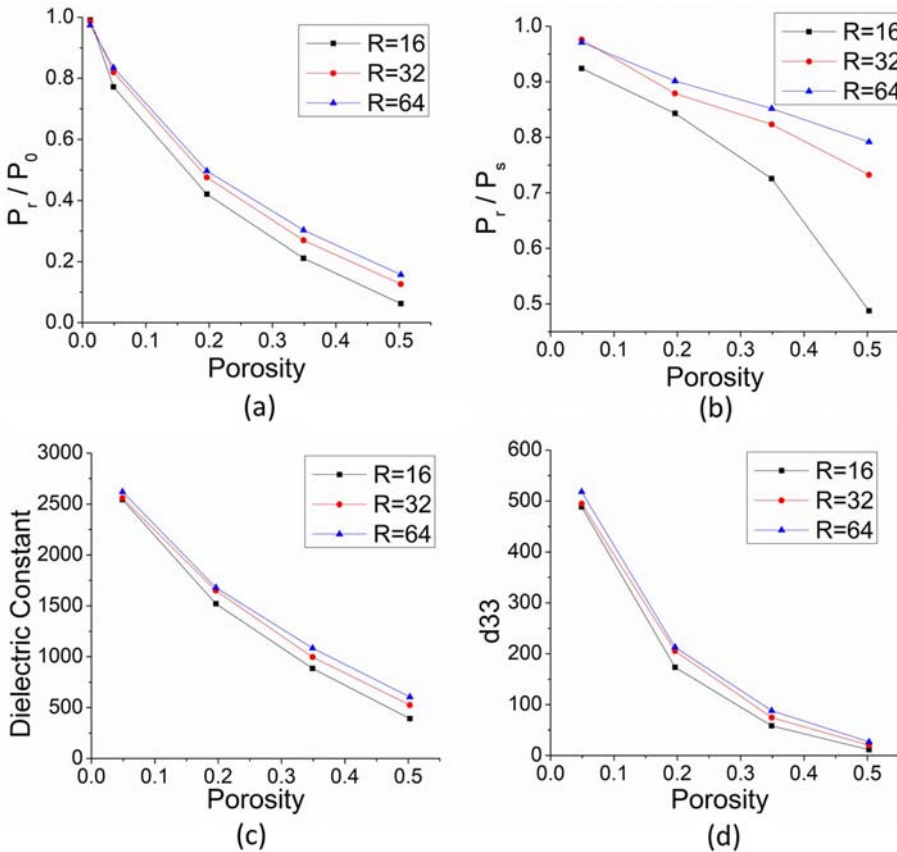


Figure 4. The remanent polarisation (a), rectangularity factor (b), dielectric constant (c) and piezoelectric coefficient (d) versus porosity calculated for various shaped porous ceramics at different porosity levels.

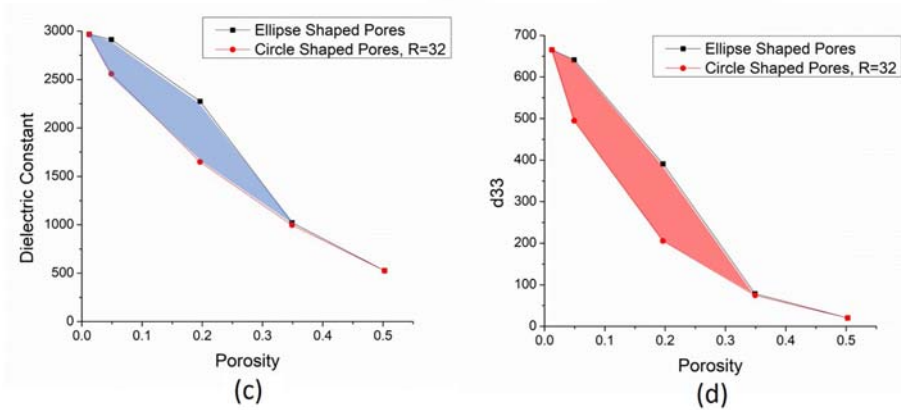
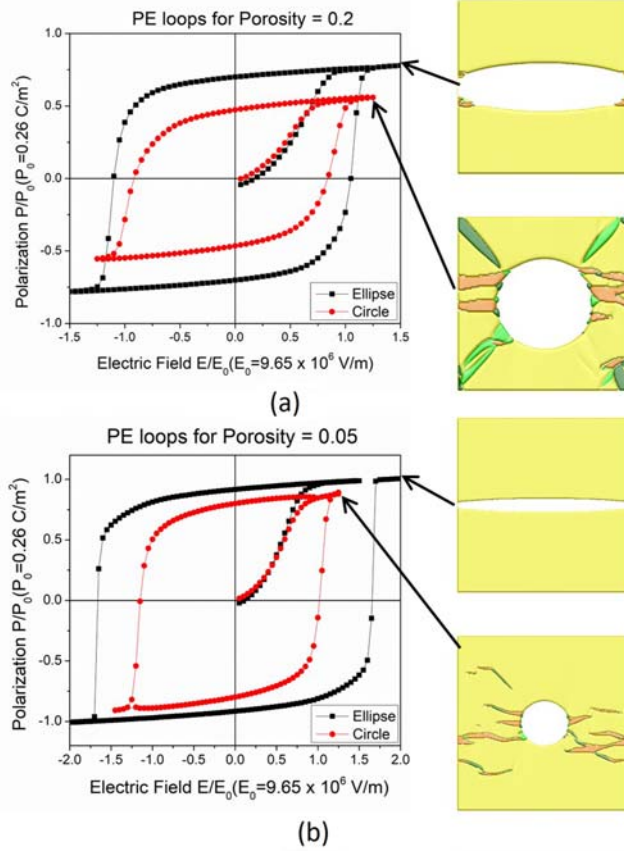


Figure 5. Hysteresis loops of BaTiO₃ with circle/ellipse shaped pores at a porosity level of 0.2 (a) and 0.05 (b). The ferroelectric domain structures at saturation are shown on the right side of the loops. (c, d) Enhanced ferroelectric properties for porous BaTiO₃ with (□) ellipse-shaped pores compared to (○) circle-shaped pores. The radius of the pores in the ferroelectrics with circle-shaped pores is fixed at 32 nm. In the ferroelectrics with ellipse-shaped pores the porosity was kept at the same level.

circle-/ellipse-shaped pores at porosity levels of 0.2 (Figure 5(a)) and 0.05 (Figure 5(b)). The radius of the circle-shaped pore is fixed at 32 nm for the two cases. At saturation, the polarisation between the pores remains zero owing to the effect of the depolarisation field (please note that periodic boundary condition is employed here). Introducing ellipse-shaped pores can decrease the volume fraction of the ferroelectric phase between the pores along the electric field direction leading to an enhancement of P_s/P_r . Furthermore, if we fixed the radius of the pores and further decrease the porosity, the number of residual domains will drop. Thus, changing the shape of pores can also improve the polarisation saturation and the coercive field.

It can be seen that an enhancement of ϵ_{33}/d_{33} was observed for ferroelectrics with ellipse-shaped pores, as indicated by the shaded region in Figure 5(c,d). It should be noted that for high-porosity ceramics, ferroelectrics with ellipse-shaped pores have a minor difference in ferroelectric properties compared to samples with round-shaped pores. In this work, for a sample at a porosity level of 20 vol% with a pore size of 32 nm, the maximum enhancements of remanent polarisation, dielectric constant and piezoelectric constant were observed to be about 47%, 38% and 90%, respectively. Furthermore, decreasing the porosity of the ceramics with ellipse-shaped pores, the enhancement of ferroelectric properties was reduced on account of the low-porosity ferroelectric structure which is close to that of the dense materials. This enhancement is also observed in porous ceramics with other pore sizes in similar porosity ranges. In this respect, the enhanced properties observed in Figure 5 may prove useful in dielectric/piezoelectric applications.

4. Summary

In summary, this paper presents a systematic phase-field simulation of the structure and ferroelectric properties of nanoporous BaTiO₃. Ferroelectric domain structures, PE loops, and related ferroelectric properties for porous BaTiO₃ with various porosity and pore size are predicted in this work. Furthermore, the effect of ellipse-shaped pores on ferroelectric properties, and the dielectric and piezoelectric constants have been analysed. The remanent polarisation, and the dielectric and piezoelectric constants were observed to be enhanced by about 47%, 38%, and 90%. It is hoped this study will be a valuable contribution to establishing reliable material properties of porous BaTiO₃ structures.

Acknowledgements

This work was supported by the outstanding young research talents program (2016) in colleges and universities of Fujian province, the Cultivating Research Program of Xiamen Institute of Technology 2018, and the Joint Research Program of Xi'an Jiaotong University and Xiamen Institute of Technology with contract No. IPE20190802 (grant number IMT2019001).

Disclosure statement

No potential conflict of interest was reported by the author(s).

Funding

This work was supported by the outstanding young research talents program (2016) in colleges and universities of Fujian province, the Cultivating Research Program of Xiamen Institute of Technology 2018, and the Joint Research Program of Xi'an Jiaotong University and Xiamen Institute of Technology with contract No. IPE20190802 (grant number IMT2019001). The author L. Du gratefully acknowledges the support of the National Natural Science Foundation of China (grant numbers 51501146, 51372197), Outstanding Youth Science Fund of Xi'an University of Science and Technology (grant number 2019YQ2-07).

ORCID

Pingping Wu  <http://orcid.org/0000-0002-7240-3760>

References

- [1] F. Gheorghiu, L. Padurariu, M. Airimioaei, L. Curecheriu, C. Ciomaga, C. Padurariu, C. Galassi, and L. Mitoseriu, *Porosity-dependent properties of Nb-doped Pb(Zr, Ti)O₃ceramics*, *J. Am. Ceram. Soc.* 100 (2017), pp. 647–658.
- [2] A.N. Rybyanets, D.I. Makarev, and N.A. Shvetsova, *Recent advances in porous piezoceramics applications*. *Ferroelectrics* 539 (2019), pp. 101–111.
- [3] Y. Zhang, M. Xie, J. Roscow, Y. Bao, K. Zhou, D. Zhang, and C.R. Bowen, *Enhanced pyroelectric and piezoelectric properties of PZT with aligned porosity for energy harvesting applications*. *J Mater Chem A Mater* 5 (2017), pp. 6569–6580.
- [4] J.I. Roscow, H. Pearce, H. Khanbareh, S. Kar-Narayan, and C.R. Bowen, *Modified energy harvesting figures of merit for stress- and strain-driven piezoelectric systems*. *Europ Phy J Spe Top* 228 (2019), pp. 1537–1554.
- [5] A. Kvasov, L.J. McGilly, J. Wang, Z. Shi, C.S. Sandu, T. Sluka, A.K. Tagantsev, and N. Setter, *Piezoelectric enhancement under negative pressure*. *Nat. Commun.* 7 (2016).
- [6] Z. Shen, H. Yan, D. Grüner, L.M. Belova, Y. Sakamoto, J. Hu, C.-W. Nan, T. Höche, and M.J. Reece, *Ferroelectric ceramics with enhanced remnant polarization by ordered coalescence of nano-crystals*. *J. Mater. Chem.* 22 (2012), pp. 23547.
- [7] C. Fang, and L. Chen, *Study of ferroelectric nanodomains and the effect of grain size in BaTiO₃ceramics*. *Philos. Mag. Lett.* 92 (2012), pp. 459–468.
- [8] W. Jiang, X. Yang, and D. Peng, *Intensity characterisation of polarisation vortex formation and evolution in ferroelectric nanofilms*. *Philos. Mag.* (2020), pp. 1–16.
- [9] J.-H. Liu, X. Chen, Y. Li, X. Guo, H.-X. Ge, and Q.-D. Shen, *Ferroelectric polymer nanostructure with enhanced flexoelectric response for force-induced memory*. *Appl. Phys. Lett.* 113 (2018).
- [10] H. Modarresi, E. Menéndez, V.V. Lazenka, N. Pavlovic, M. Bisht, M. Lorenz, C. Petermann, M. Grundmann, A. Hardy, M.K. Van Bael, M.J. Van Bael, A. Vantomme, and K. Temst, *Morphology-induced spin frustration in granular BiFeO₃ thin films: origin of the magnetic vertical shift*. *Appl. Phys. Lett.* 113 (2018).

- [11] Y. Ni, and A.G. Khachatryan, *Phase field approach for strain-induced magnetoelectric effect in multiferroic composites*. J. Appl. Phys. 102 (2007), pp. 113506.
- [12] R. Kargupta, and T. Venkatesh, *Electromechanical response of porous piezoelectric materials*. Acta Mater. 54 (2006), pp. 4063–4078.
- [13] A. Castro, P. Ferreira, B.J. Rodriguez, and P.M. Vilarinho, *The role of nanoporosity on the local piezo and ferroelectric properties of lead titanate thin films*. J. Mater. Chem. C 3 (2015), pp. 1035–1043.
- [14] R. Khachatryan, S. Zhukov, J. Schultheiß, C. Galassi, C. Reimuth, J. Koruza, H. von Seggern, and Y.A. Genenko, *Polarization-switching dynamics in bulk ferroelectrics with isometric and oriented anisometric pores*. J. Phys. D: Appl. Phys. 50 (2017).
- [15] C. Ming, T. Yang, K. Luan, L. Chen, L. Wang, J. Zeng, Y. Li, W. Zhang, and L.-Q. Chen, *Microstructural effects on effective piezoelectric responses of textured PMN-PT ceramics*. Acta Mater. 145 (2018), pp. 62–70.
- [16] Y. Zhang, J. Roscow, R. Lewis, H. Khanbarez, V.Y. Topolov, M. Xie, and C.R. Bowen, *Understanding the effect of porosity on the polarisation-field response of ferroelectric materials*. Acta Mater. 154 (2018), pp. 100–112.
- [17] G. Martínez-Ayuso, M.I. Friswell, H. Haddad Khodaparast, J.I. Roscow, and C.R. Bowen, *Electric field distribution in porous piezoelectric materials during polarization*. Acta Mater. 173 (2019), pp. 332–341.
- [18] L. Van Lich, T. Shimada, J. Wang, and T. Kitamura, *Self-ordering of nontrivial topological polarization structures in nanoporous ferroelectrics*. Nanoscale. 9 (2017), pp. 15525–15533.
- [19] H. Chen, X. Hou, J. Chen, S. Chen, P. Hu, H. Wu, J. Wang, and J. Zhu, *Large electro-strain induced by reversible domain switching in ordered ferroelectric nanostructures with optimized geometric configurations*. Nanotechnology 31 (2020), pp. 335714.
- [20] X. Hou, H. Li, T. Shimada, T. Kitamura, and J. Wang, *Effect of geometric configuration on the electrocaloric properties of nanoscale ferroelectric materials*. J. Appl. Phys. 123 (2018), pp. 124103.
- [21] K.A. Khan, and M.A. Khan, *3-3 piezoelectric metamaterial with negative and zero Poisson's ratio for hydrophones applications*. Mater. Res. Bull. 112 (2019), pp. 194–204.
- [22] L. Shu, R. Liang, Y. Yu, T. Tian, Z. Rao, and Y. Wang, *Unique elastic, dielectric and piezoelectric properties of micro-architected metamaterials*. J. Mater. Chem. C 7 (2019), pp. 2758–2765.
- [23] J.I. Roscow, Y. Zhang, M.J. Kraśny, R.W.C. Lewis, J. Taylor, and C.R. Bowen, *Freeze cast porous barium titanate for enhanced piezoelectric energy harvesting*. J. Phys. D: Appl. Phys. 51 (2018), pp. 225301.
- [24] H. Zhao, P. Wu, L. Du, and H. Du, *Effect of the nanopore on ferroelectric domain structures and switching properties*. Comput. Mater. Sci. 148 (2018), pp. 216–223.
- [25] A.G. Khachatryan, *Theory of Structural Transformations in Solids*, Wiley, New York, 2008.